Experimental studies of magnetic reconnection*

M. R. Brown†
Department of Physics and Astronomy, Swarthmore College, Swarthmore, Pennsylvania 19081-1397

(Received 12 November 1998; accepted 10 February 1999)

Laboratory magnetic reconnection experiments have been performed for nearly 20 years. Elegant experiments by Stenzel and Gekelman [R. L. Stenzel and W. Gekelman, Phys. Rev. Lett. **42**, 1055 (1979); W. Gekelman and R. L. Stenzel, Phys. Rev. Lett. **54**, 2414 (1985)] focused on the measurement of field quantities with a single movable probe in a highly reproducible plasma. Observations included a very thin current sheet (on the order of c/ω_{pe}), accelerated electrons, and whistler waves. The argon ions were unmagnetized in these experiments. Recent magnetohydrodynamic (MHD) experiments by Yamada and Ono have used merging plasmoids [M. Yamada, Y. Ono, A. Hayakawa, M. Katsurai, and F. W. Perkins, Phys. Rev. Lett. **65**, 721 (1990); Y. Ono, M. Yamada, T. Akao, T. Tajima, and R. Matsumoto, Phys. Rev. Lett. **76**, 3328 (1996)] and have measured three dimensional effects and ion acceleration. We have observed correlations between magnetic reconnection and energetic ion flow events with merging force free spheromaks at the Swarthmore Spheromak Experiment (SSX) [T. W. Kornack, P. K. Sollins, and M. R. Brown, Phys. Rev. E **58**, R36 (1998)]. The reconnection layer is measured with linear and two dimensional probe arrays and ion flow is directly measured with a retarding grid energy analyzer. Flow has been measured both in the plane of the reconnection layer and out of the plane. The outflow velocity is nearly Alfvénic in the reconnection plane and the scale of the magnetic structures is consistent with collisionless reconnection theories (on the order of c/ω_{pi}). Results from the two dimensional array show the formation of magnetic islands correlated with super-Alfvénic ions accelerated normal to the layer. © *1999 American Institute of Physics.* [S1070-664X(99)96805-2]

I. INTRODUCTION

Magnetic reconnection refers to events in which magnetic flux is locally annihilated resulting in a global change in magnetic topology. In astrophysical contexts, magnetic reconnection occurs when parcels of magnetofluid with oppositely directed flux are merged (for example, when two solar flares are brought together or when a single loop of magnetofluid is twisted or distorted). Intense current sheets are formed at the interface of the merging parcels which convert magnetic energy to heat and energetic particles. In the laboratory, magnetic reconnection occurs when columns of magnetofluid become overly sheared (due to high current) or when separate bundles of magnetofluid are merged.

The paradigm for magnetic reconnection is the merger of two parcels of magnetofluid with anti-parallel flux (see Fig. 1). In the rest frame of either parcel, there is no electric field (and no velocity); simply magnetofluid at rest. The velocities of the parcels stagnate to zero at a neutral sheet which defines a new frame of reference. In the rest frame of the neutral sheet, the parcels are moving in towards the layer. If $E'=0$ in the magnetofluid rest frame, then $E+v\times B=0$ outside the layer in the rest frame of the neutral sheet (by a Lorentz transformation). The role of the electric field is nondissipative (i.e., purely convective) outside the layer. When the parcels stagnate, the electric field becomes dissipative inside the layer and $E=\eta J$. This directed electric field is capable of heating plasma and accelerating charged particles to high energies.

The transition from nondissipative drift to a dissipative current sheet and the mechanism for dissipation and breaking of magnetic field lines is a subject of considerable debate. The key idea is that the thickness of the layer adjusts to a scale such that convection is balanced by diffusion. The magnetic lines of force then lose their identity in the layer so that a line associated with one parcel of magnetofluid becomes associated with the other.

It is becoming clear that the sun (and likely other astrophysical magnetofluid) is able to generate and annihilate magnetic flux at all scales. The generation mechanism is evidently some kind of dynamo. There is growing evidence that annihilation via magnetic reconnection plays a crucial role in particle acceleration and heating in astrophysical plasmas. Recently, the Yohkoh satellite has produced dramatic images of solar flares correlating x-ray, magnetic and particle data for the first time. Observations made with the Yohkoh hard x-ray and soft x-ray telescopes have identified the reconnection region at the top of the flare as the site of particle acceleration.[1] Shibata *et al.*[2] detected jets of upward flowing plasma above the Masuda flare at close to the Alfvén speed v_{Alf} providing further evidence of reconnection and conversion of magnetic energy to kinetic energy in flares. Doppler shift measurements on the Solar Heliospheric Observatory (SOHO) ultraviolet spectrometer show evidence of bidirectional Alfvénic jets in the reconnection plane.[3] Laboratory experiments can now begin to shed some light on these observations.

*Paper C2TV.1 Bull. Am. Phys. Soc. **43**, 1661 (1998).
†Tutorial speaker.

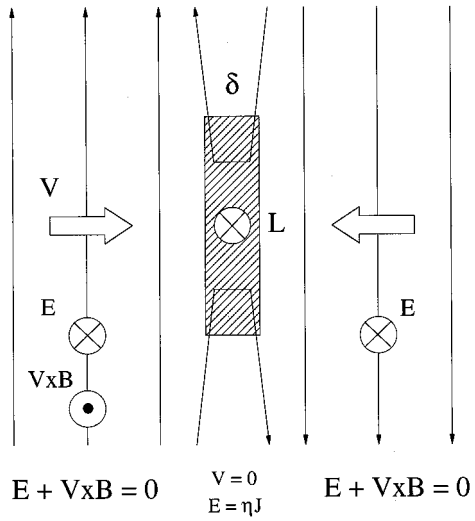

FIG. 1. Magnetic reconnection paradigm. Merging parcels of magnetofluid have no electric field in their respective rest frames. By special relativity, in any other frame (in particular, that of the neutral sheet) the relation $E+v\times B=0$ holds. At the neutral sheet, the velocities stagnate to zero so the role of the electric field becomes dissipative.

In Sec. II, key aspects of reconnection theory are summarized. In Sec. III results from two important sets of reconnection experiments [one at the University of California, Los Angeles (UCLA), the other at Tokyo/Princeton] are reviewed. In Sec. IV, recent results from the Swarthmore Spheromak Experiment are reported.

II. SUMMARY OF RECONNECTION THEORIES

Predictions of the structure and thickness of the reconnection layer depend sensitively on the model used. If parcels of magnetofluid of macroscopic scale L and with oppositely directed magnetic flux are merged at a velocity of v_{in} then a boundary layer of thickness δ is formed where the opposing flux is annihilated (see Fig. 1). The resistive magnetic induction equation can be written by taking the curl of the magnetohydrodynamic (MHD) Ohm's law $(E+v\times B=\eta J)$:

$$\frac{\partial B}{\partial t}=\nabla\times(v\times B)+\frac{\eta}{\mu_0}\nabla^2 B.$$

Resistive MHD predicts that in steady state the two terms on the right-hand side balance. Writing $\nabla\sim 1/\delta$ as an inverse scale length across the layer, this condition can be written

$$R_m=\frac{\mu_0 v_{in}\delta}{\eta}=1,$$

where R_m is the magnetic Reynolds number (the ratio of convection to diffusion) based on the inflow velocity and the thickness of the layer. The assumptions of incompressibility and energy conservation yield

$$v_{out}=\frac{L}{\delta}v_{in}=v_{Alf}.$$

The scales and velocities are therefore related by

$$\frac{L}{\delta}=\frac{v_{out}}{v_{in}}=\sqrt{S},$$

where S is the Lundquist number based on the macroscopic scale L ($S=R_m$ if v_{Alf} is used for the velocity). Since $S\propto\eta^{-1}$, resistive MHD predicts[4,5] that the thickness of the layer vanishes like $1/\sqrt{S}$. Outside the layer, the $v\times B$ term in Ohm's law dominates resistivity so the role of the electric field is to generate nondissipative $E\times B$ flow into the layer (slowly) and out of the layer (rapidly). Since the outflow is limited to the Alfvén speed (by energy conservation), the reconnection rate is limited by thickness of the layer. Inside the layer, the electric field is dissipative but can accelerate charged particles to high energies.

It has recently been shown[6] that in the collisionless limit of large S (and small η) Hall dynamics and electron inertia govern the scale of reconnection. Clearly, kinetic effects must be considered at small scales. Electron and ion dynamics decouple on scales smaller than the ion inertial length c/ω_{pi} and the thickness of the layer is clamped by ion inertia. Electron dynamics generate an inner scale c/ω_{pe} where the frozen-in flux constraint is broken and reconnection occurs. Below the c/ω_{pi} scale we expect the single fluid MHD model to fail and kinetic effects to dominate. Dynamics at the c/ω_{pe} scale where only the electrons are magnetized are often referred to as electron MHD (or EMHD).

Two dimensional resistive MHD simulations[7] predict acceleration of a few particles to super-Alfvénic velocities normal to the layer in addition to the Alfvénic flow across the layer. The super-Alfvénic particles are trapped in ''magnetic bubbles'' for a few Alfvén times and are accelerated by the self-consistent electric field at the O-point. This energetic tail is predicted to be convected across the layer at v_{Alf}. Collisionless two-and-one-half dimensional (2-1/2 D) hybrid simulations[8] also predict ion beams (as well as in-plane Alfvénic flow) and significant out-of-plane magnetic fields. As the magnetic flux and electron fluid decouple at the inner scale (c/ω_{pe}) an out of plane super-Alfvénic jet of electron fluid is seen. The electron jet drags flux out of the plane to produce out-of-plane magnetic fields. Much of these interesting dynamics remain to be seen experimentally.

III. RECONNECTION EXPERIMENTS

A. UCLA experiments

The first detailed measurements of magnetic reconnection were performed nearly 20 years ago by Stenzel and Gekelman at UCLA[9] and proceeded through the 1980's.[10,11] Experiments were performed in a large linear device and plasma was produced by a large (1 m diameter) cathode discharge. The pulsed plasma ($n_e\cong 10^{12}$ cm^{-3}, $T_e\cong 10T_i=5-30$ eV) was immersed in a uniform magnetic field ($B_0\cong 10$ G). Since $\rho_i\cong R_{chamber}$, the ions are unmagnetized in this experiment.

There were at least two schemes for formation of the reconnection geometry. First, parallel currents could be pulsed through a pair of plates above and below the plasma (see Fig. 2). An induced current flows in the plasma anti-

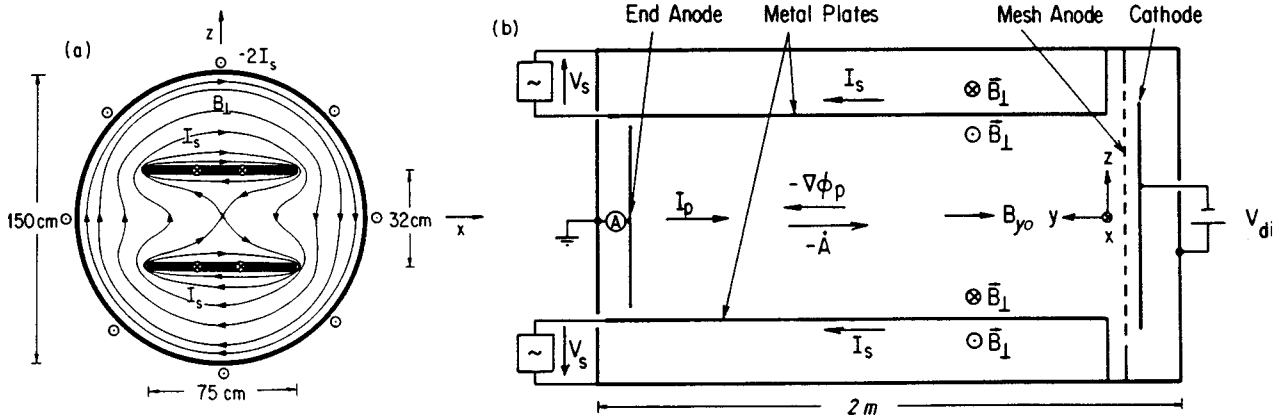

FIG. 2. Schematic of the UCLA reconnection experiment. (a) Cross-sectional view showing transverse vacuum magnetic fields. (b) Side view with characteristic fields and currents.

parallel to the plate current. In a second scheme, the discharge current was masked to allow only a sheet current to flow. Both schemes yielded similar results.

The key technique in the UCLA experiments was to perform careful point measurements of field quantities (**B**, **E**, **v**, n_e, and T_e) using single probes and to rely on the reproducibility of the discharge. The results of several measurements at one location were averaged (25 to 80 discharges) before the probe was moved. The time between discharges was short (2 s) so that hundreds of spatial locations and thousands of discharges could be measured during a run.

The main result[12] was that the average magnetic field topology evolved to a classic double Y geometry with a current sheet thickness intermediate between the electron inertial and ion gyroradius scales ($c/\omega_{pe} \leqslant \delta \leqslant \rho_i$) [see Fig. 3(a)]. In addition, the distinctive outflow in the reconnection plane at the Alfvén speed was also verified [see Fig. 3(b)].

Electron temperature and density were measured throughout the reconnection region using rapidly swept electrostatic probes.[13,14] The kinetic pressure ($p=nkT$) and the magnetic pressure ($B^2/2\mu_0$) can be plotted separately and compared [see Fig. 4; note that the axis in (b) should be labelled 10^{-6}]. The total pressures were shown to be com-

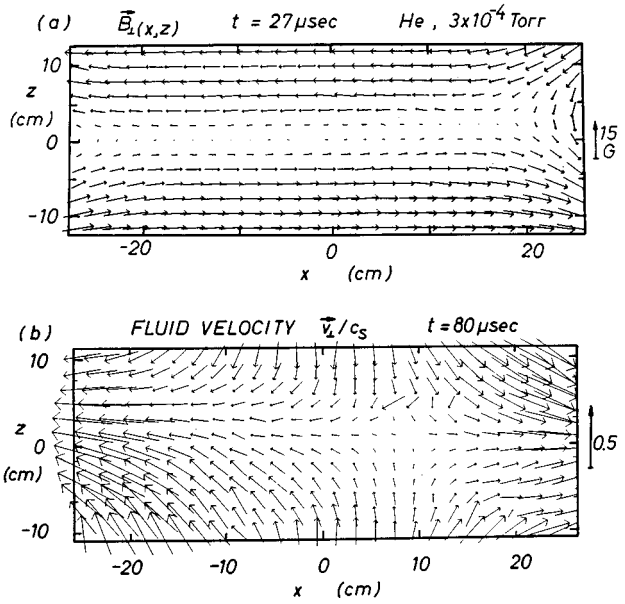

FIG. 3. Measured vector fields in the UCLA device (a) $\mathbf{B}_\perp$ and (b) $\mathbf{v}_\perp$. Note the classic double Y topology, with current sheet thickness on the order of c/ω_{pe} and that the outflow speed is nearly Alfvénic ($v_{Alf} \approx c_s$).

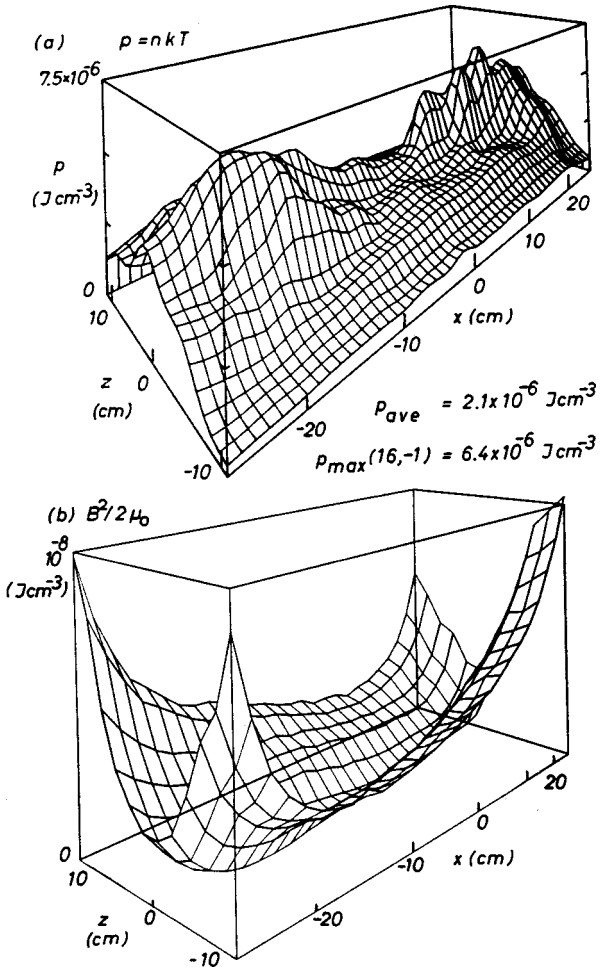

FIG. 4. (a) Kinetic ($p=nkT$) and (b) magnetic pressure ($B_\perp^2/2\mu_0$) in the UCLA device. The total pressures are comparable ($\beta \approx 1$) but not in equilibrium. The axis in (b) should be labeled 10^{-6}.

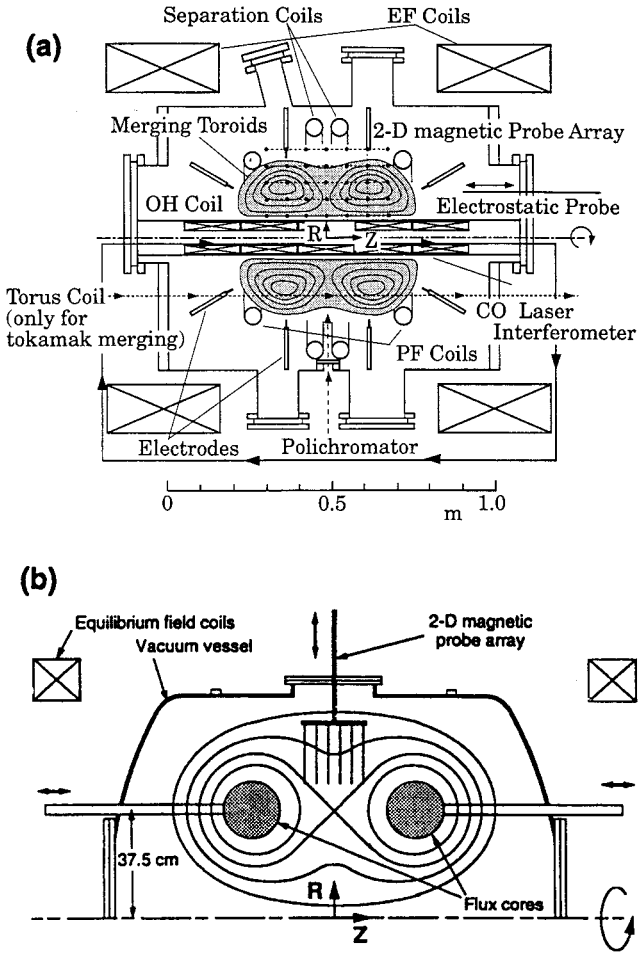

FIG. 5. (a) Schematic of the Tokyo TS-3 device and (b) the Princeton MRX device showing locations of probe arrays and formation apparatus.

parable (as expected since $\beta \cong 1$) but locally the pressure is not balanced. The lack of equilibrium results in an acceleration of the plasma out of the neutral sheet. In addition, the total MHD force density ($\mathbf{f}=\mathbf{J}\times\mathbf{B}-\nabla p$) can be compared with the time derivative of the fluid momentum. It was found that $\mathbf{f}$ was much larger than the fluid momentum change. The difference was determined to be due to anomalous scattering of the flow off turbulent fluctuations.

The source of the turbulent fluctuations were determined with careful plasma kinetic measurements including the electron distribution function and wave activity.[15] Autocorrelations and cross-correlation between two probes were measured throughout the experimental volume. The wavelength of the waves excited by reconnection activity ($\lambda \sim 10$ cm) was consistent with whistler waves. The structure of ambient waves was compared to that of test waves and it was determined that the magnetic turbulence was a random ensemble of obliquely propagating whistlers. Measurements of $f(v,r,t)$ showed anisotropies in the form of runaway electrons.[16] The effective resistance of the plasma was influenced by the collisionality of the runaways (and not the average temperature of the bulk electrons). A large fraction of the current was carried by runaway electrons which are less collisional than the bulk electrons. In addition, anisotropies

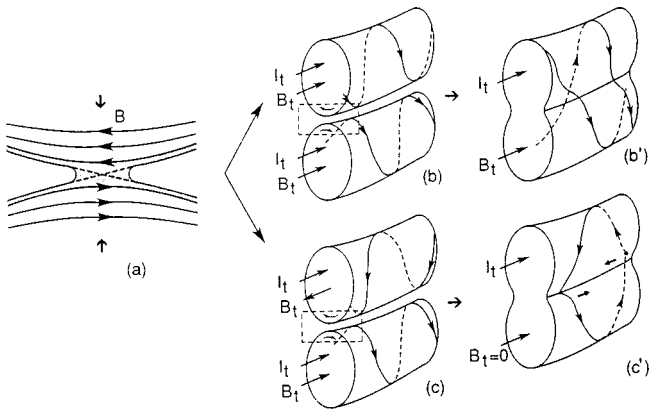

FIG. 6. Three-dimensional effects of magnetic reconnection. (a) The local 2D poloidal picture is modified by the addition of a toroidal field (b) and (c).

in $f(v,r,t)$ drive whistler turbulence which (as noted above) affects force balance and tends to increase the effective resistivity of the plasma.

The UCLA experiments were performed at the c/ω_{pe} scale, which is where we expect $\beta \cong 1$, and in the collisionless case, where we expect the frozen in flux condition to be broken. These studies focused on the inner scale of magnetic reconnection. Subsequent experiments at Tokyo, Princeton, and Swarthmore are unable to resolve this inner scale, but reveal some similarities. The key to the future understanding of magnetic reconnection will be in focusing on kinetics (waves and particles) as the UCLA group has done.

B. Tokyo/Princeton experiments

In the 1990's, magnetic reconnection experiments moved fully into the MHD regime beginning with experiments of Yamada and Ono at the University of Tokyo.[17] The key differences between these experiments and the earlier UCLA experiments were (1) the ions (protons) are fully magnetized $\rho_i \ll R_{chamber}$, (2) arrays of dozens of magnetic probes are used on a single discharge, (3) the current sheet is formed and reconnection proceeds by merging separate bundles of magnetized plasma, (4) the measurements resolve the c/ω_{pi} scale but not the c/ω_{pe} scale, and (5) the reconnection geometry is fully three dimensional.

A variety of formation schemes have been employed (Fig. 5). The Tokyo experiment has focused on ''$z-\theta$'' formation. The Princeton Magnetic Reconnection Experiment (MRX) employs a ''flux-core'' formation scheme. In both cases, gas is ionized *in situ* so that plasma is generated with imbedded magnetic flux (forming the magnetofluid). Typical plasma parameters include $n_e \cong 10^{14}$ cm^{-3}, $T_e \cong T_i = 10-30$ eV and have a typical magnetic field $B_0 \leqslant 1$ kG.

There are several important results from this work. Yamada and Ono have pointed out the importance of three-dimensional effects on the reconnection rate.[17–19] The idea is that the simple two dimensional (2D) Sweet–Parker picture is modified by the addition of magnetic flux in the third dimension (see Fig. 6). If the added field is in the same direction in both the upper and lower flux bundles then the reconnection angle is less than 180 degrees and the recon-

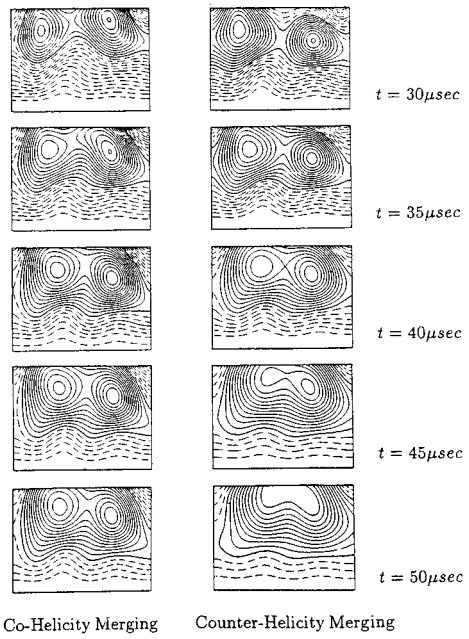

FIG. 7. Evolution of the poloidal flux for (a) co-helicity and (b) counter-helicity merging in the Tokyo TS-3 device.

nection rate is reduced. An interpretation is that the work required to compress the added flux slows the reconnection rate. If the added field is in opposite directions (top and bottom) then the reconnection angle stays near 180 degrees and the reconnection rate is comparable to the 2D case. Viewed in terms of magnetic helicity, the first case is referred to co-helicity and the second to counter-helicity [the sign of helicity can be written $(\mathbf{I_t}\cdot\mathbf{B_t})/(I_tB_t)$]. The experimental results (Fig. 7) show that merging is much more rapid in the counter-helicity case. In other words, the reconnection rate, which is just the electric field from Faraday's law, is higher if the local reconnection angle is close to 180 degrees. Except for the relative sign of helicity, these two discharges were identical.

Associated with the higher reconnection rates in counter-helicity merging, they have also observed ion heating and acceleration by Doppler broadening and shifts of line emission (H_β, C_{II}).[20] Figure 8 shows the measured ion temperature profile from Doppler broadening of the H_β line. Note that the characteristic time for ion heating from 10 eV to 200 eV is only about 10 μs (a few Alfvén times).

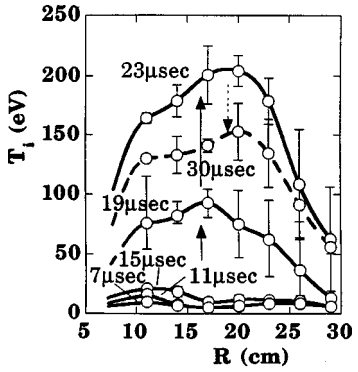

FIG. 8. Evolution of the radial ion temperature profile T_i on the TS-3 midplane during counter-helicity merging.

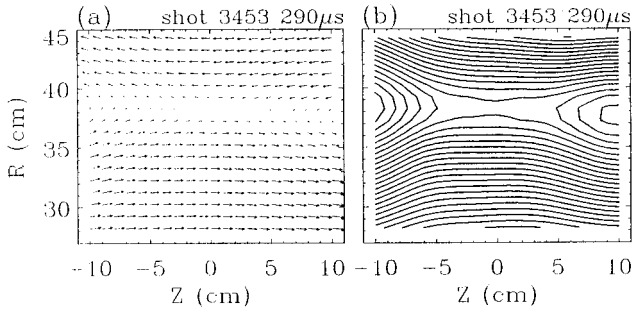

FIG. 9. Driven reconnection in the MRX device: Data from a 2D magnetic probe array on a single shot. The double Y topology is observed during null helicity merging. Note the similarity to Fig. 3.

Both Y- and O-shaped structures have been observed in the reconnection layer in the MRX device[21]. The double Y topology is observed in ''null-helicity'' merging (purely two dimensional structure with no toroidal field at all, Fig. 9) while O-points are observed during co-helicity merging. Recent results indicate that classical resistivity is insufficient to explain their observed reconnection rates.[22] However, if the effects of compressibility, pressure differences between up and down stream, and an effective resistivity (due to turbulence) are included, a modified version of the Sweet–Parker theory can explain their results. Note the general similarity of Fig. 9 to the corresponding UCLA result (Fig. 3). The key difference is that a few cm correspond to the ion c/ω_{pi} scale in the MRX plasma while a few cm correspond to the electron c/ω_{pe} scale in the much less dense UCLA device. There appears to be a self-similarity at both scales.

IV. SWARTHMORE SPHEROMAK EXPERIMENT

We are able to generate force-free spheromaks with magnetized plasma guns at the Swarthmore Spheromak Experiment (SSX)[23] and merge them coaxially. Both one and two dimensional magnetic data are recorded in the plane of intersection of the spheromaks. We observe a rapid formation of a reconnection layer (within a few Alfvén transit times of spheromak formation) followed by the appearance of Alfvénic (suprathermal) ion flow at an electrostatic energy analyzer.[24] We have made ion flow measurements both in and out of the reconnection plane and the flow appears to be predominantly in the plane containing the reconnecting field, although there is some evidence of super-Alfvénic ion flux normal to the layer. The thickness of the reconnection layer is consistent with the collisionless two fluid prediction of $\delta \approx c/\omega_{pi}$.

The key difference between this and previous work is that the magnetofluid is generated by plasma guns away from the interaction region. Neutral gas is introduced at the remote guns but only fully ionized plasma and imbedded magnetic fields convect into the interaction region. Triple probe measurements[25] yield $T_e \approx$ 20 eV and $n_e \approx 10^{14}$ cm^{-3} for SSX plasmas and our average magnetic field is 500 G. These

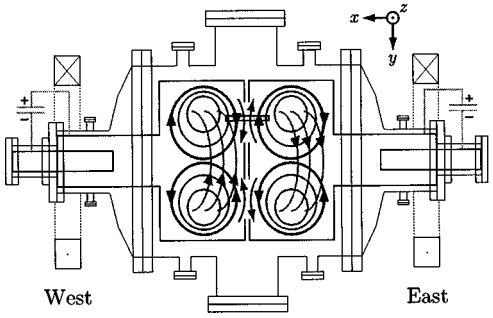

FIG. 10. Schematic of the SSX experiment showing both guns with two large flux conservers to allow reconnection studies. Depicted is the magnetic field structure for a left- (right-) handed spheromak in the east (west) flux conserver. The view is the x-y plane from above.

values give $c/\omega_{pi} \approx 2$ cm and $S \lesssim 1000$ and predict a resistive reconnection layer thickness $\delta < 1$ cm. If $T_i \simeq T_e$ then $\rho_i \leqslant 1$ cm. The collisional mean free path is ≈ 10 cm and the Alfvén speed is about 10^7 cm/s.

Figure 10 shows the experimental arrangement with the orientation of the linear magnetic probe array. For all the data presented here the spheromaks had opposite magnetic helicity, i.e., both the poloidal and toroidal fields were opposed at the reconnection layer. Counterhelicity merging of coaxial spheromaks corresponds locally to a nearly two dimensional reconnection layer.[17] We are able to change the orientation of the poloidal flux in both the east and west spheromak on subsequent shots (while keeping the toroidal orientation in each fixed). A switch from right–left merging to left–right merging corresponds to a $\approx 90°$ rotation of the local 2D reconnection plane. In this way we can arrange to have our energy analyzer diagnostic either in or out of the reconnection plane.

The retarding grid energy analyzer (RGEA) consists of a series of grids to suppress electrons (-10 V) and discriminate ions according to their energy (0–100 V) in front of a biased Faraday cup for ion collection (-30 V). The analyzer sits outside the flux conservers (about 50 cm away) and looks between them such that it measures only particles escaping the reconnection layer. Spheromaks communicate

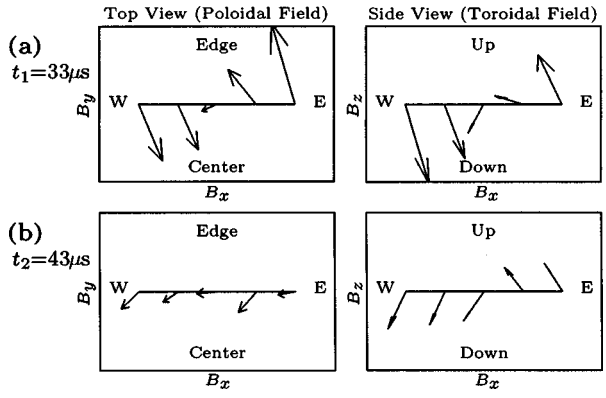

FIG. 11. SSX reconnection data (a) t_1 before annihilation, (b) t_2 after annihilation 10 μs later. The two views are projections of the magnetic field vectors into the horizontal (x-y) and vertical (x-z) planes. Probe separation is 2 cm. $B_{max} \simeq 1100$ G.

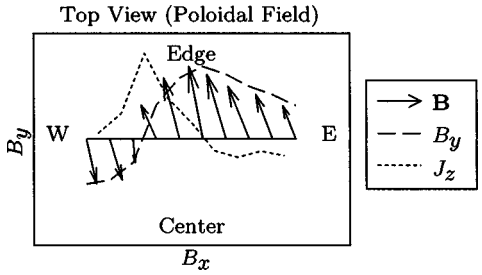

FIG. 12. Details of the SSX reconnection layer in the horizontal (x-y) plane and the inferred $J_z \sim \partial B_y/\partial x$ at about t_1. Probe separation is 1 cm. $B_{max} \simeq 930$ G.

across a 2 cm gap via large (12 cm by 9 cm) chevron-shaped slots cut in the back of each flux conserver. Since the spheromaks are formed by external plasma guns, the stray magnetic field and neutral gas levels in the gap are small. The slots force a macroscopic scale of 12 cm (comparable to the spheromak minor radius). The remaining copper in the back walls provide stability against tilting.

In Fig. 11 we present two projections of the magnetic field vectors (in the x-y and x-z planes) at 5 locations across the layer at two different times. The probe separation is 2 cm. For this shot, the east (west) spheromak had left- (right-) handed helicity such that the energy analyzer is in the reconnection plane (as depicted in Fig. 10). Note that at $t_1 = 33$ μs [Fig. 11(a)] a reconnection layer has formed with opposed poloidal and toroidal fields (the magnitude of the largest magnetic field vector is about 1100 G). The thickness of the reconnection layer is evidently about 2 cm consistent with our value of c/ω_{pi}. At $t_2 = 43$ μs [Fig. 11(b)] much of the poloidal flux has been annihilated. Note again that the characteristic time for flux annihilation and energy conversion is very rapid (only about 10 μs or a few Alfvén times).

We have verified the thickness of the layer with a higher resolution probe array (probe separation of 1 cm). In Fig. 12 we show the poloidal field and the inferred $J_z \sim \partial B_y/\partial x$ for a shot similar to that shown in Fig. 11 at t_1. Here the width of the current layer is $\simeq 2$ cm consistent with c/ω_{pi}.

Correlated with this flux annihilation event is a delayed burst of plasma flow across the layer. In Fig. 13 we present the magnetic energy density around the layer [Fig. 13(a)] and the signal on the RGEA (proportional to energetic ion flux)

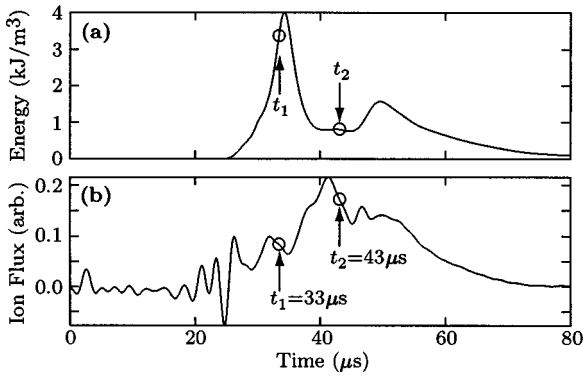

FIG. 13. Time history of the shot in Fig 11. (a) Local magnetic energy density and (b) energetic ion flux.

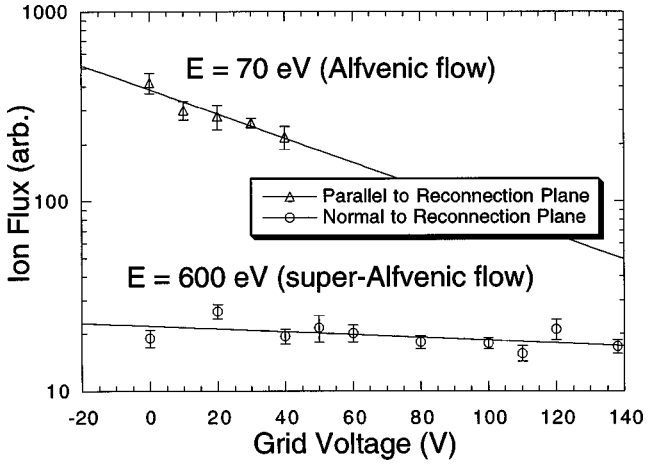

FIG. 14. Retarding energy analyzer scan in the SSX device. Top: merging spheromaks (in-plane), Alfvénic ions, $\bar{E} = 70$ eV. Bottom: merging spheromaks (out-of-plane), super-Alfvénic ions, $\bar{E} = 600$ eV. The data are fit with a simple one parameter model.

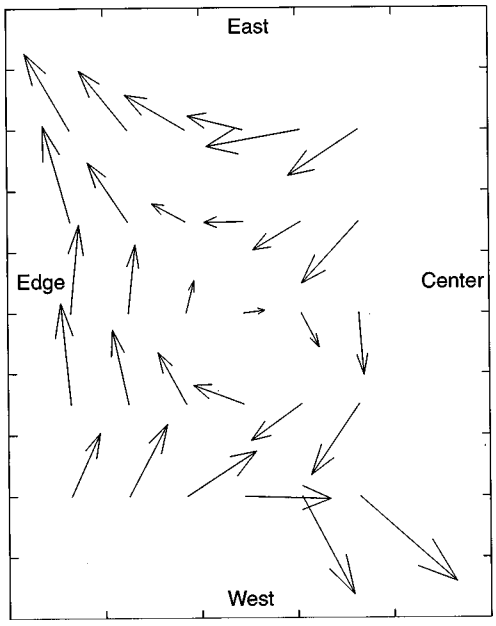

FIG. 15. Data from a 2D magnetic probe array on a single SSX shot. The O-point is observed during counter-helicity merging and may play a role in confining energetic particles. Probe resolution is 2 cm.

[Fig. 13(b)] for the same shot as in Fig. 11. The magnetic energy density is defined $W=(1/N)\Sigma B^2/2\mu_0$ where the sum extends over the $N=5$ probe locations. We note a peak in the magnetic energy density as the layer is formed followed by a peak in the energetic ion flux. The delay between the annihilation of magnetic flux (drop in magnetic energy) and the appearance of energetic ions 50 cm away is about 5 μs giving an ion flow velocity of about v_{Alf} for this event (10^7 cm/s). The later peak is due to a recovery of the spheromak fields and reestablishment of the layer.

We have performed scans of the retarding grid voltage to determine the average energy of the peak ion flux. In Fig. 14 we present escaping ion flux data as a function of energy for (top) two merging spheromaks with the detector in the reconnection plane and (bottom) merging spheromaks with the detector viewing normal to the plane. We have fit the data to the simple model $\Gamma=\Gamma_0 \exp(-V/\bar{E})$ where $\bar{E}$ is the average energy. The in-plane reconnection particle flux is at significantly higher average energy ($\bar{E}=70$ eV) than the thermal ions ($\bar{E}=30$ eV). The velocity of 70 eV protons corresponds to the Alfvén speed at $n_e \approx 10^{14}$ cm^{-3} and $B \approx 500$ G consistent with our probe measurements so the in-plane flow is due to Alfvénic and not thermal ions.

In order to illustrate the difference between particle dynamics across the layer versus normal to the layer, we have conducted a preliminary search for super-Alfvénic ion flux normal to the layer as predicted by Matthaeus *et al.*[7] For this experiment, we added a new port that was angled to directly view the reconnection plane from above. The RGEA was well removed from the experimental region (over 1 m away) so that only high energy ions could be expected to traverse the distance. We find a very low flux of ions at very high energy. The retarding grid had almost no effect on the collected current (see Fig. 14, bottom) and the pulse of ions arrived within a microsecond after reconnection. While there is significant scatter from shot-to-shot fluctuations, it is clear that the flux of ions normal to the plane of reconnection is at higher average energy than the flux of ions in the plane of reconnection. These results are preliminary and the model is crude. More systematic studies of the ion energy analyzed with more sophisticated models (including drift and nonthermal effects) will be performed both at SSX and elsewhere.

We have implemented a two dimensional magnetic probe array (measuring **B** on a 5 by 6 grid with 2 cm resolution). Our measurements confirm the earlier 1D array results (both the timing and spatial structure) but reveal an interesting feature. We see the formation of an O-point within 10 μs after merging (see Fig. 15). O-points have been observed in the MRX experiment but only in the case of co-helicity merging. We observe the formation of an O-point during counter-helicity merging, indicating that such structures might be a ubiquitous feature of magnetic reconnection. Future studies will attempt to correlate the appearance of the super-Alfvénic ion flux with the appearance of the O-point. We also plan to completely remove the stabilizing copper wall and therefore remove any influence the conducting boundary might have on reconnection dynamics.

To summarize, we have experimentally observed correlated magnetic reconnection and energetic ion events at SSX. The highest flux events are jets localized to the plane containing the reconnecting poloidal flux and are consistent with Alfvénic flow. The thickness of the layer is consistent with two fluid collisionless theory and not consistent with the predictions of resistive MHD.

Future work on magnetic reconnection will focus on three dimensional effects and particle acceleration mechanisms. It is becoming clear that resistive MHD is an insufficient model to explain experimental results. Collisionless models incorporating Hall effects and electron inertia will have to be employed. In addition, kinetic effects such as particle distributions and fluctuations (both Alfvénic and whistler) need to be measured.

ACKNOWLEDGMENTS

This work was performed in collaboration with C. Geddes, T. Kornack, P. Sollins, V. Lukin, D. Auerbach, and A. Carlisle (Swarthmore), W. Matthaeus (Bartol), D. Schnack (Science Applications Incorporated), and S. Paul (Princeton). Special thanks to S. Palmer and D. Radcliff for assistance with the apparatus.

This work was performed under Department of Energy (DOE) Grant No. DE-FG02-97ER54422. M.R.B. is a DOE Junior Faculty Investigator.

[1]S. Masuda, T. Kosugi, H. Hara, S. Tsuneta, and Y. Ogawara, Nature (London) **371**, 495 (1994).
[2]K. Shibata, Astrophys. J. **451**, 83 (1995).
[3]D. E. Innes, B. Inhester, W. I. Axford, and K. Wilhelm, Nature (London) **386**, 811 (1997).
[4]P. A. Sweet, *Electromagnetic Phenomena in Cosmical Physics*, edited by B. Lehnert (Cambridge University Press, London, 1958).
[5]E. N. Parker, J. Geophys. Res. **62**, 509 (1957).
[6]D. Biskamp, E. Schwartz, and J. F. Drake, Phys. Rev. Lett. **75**, 3850 (1995).
[7]W. H. Matthaeus, J. J. Ambrosiano, and M. L. Goldstein, Phys. Rev. Lett. **53**, 1449 (1984).
[8]M. A. Shay, J. F. Drake, R. E. Denton, and D. Biskamp, J. Geophys. Res. **103**, 9165 (1998).
[9]R. L. Stenzel and W. Gekelman, Phys. Rev. Lett. **42**, 1055 (1979).
[10]W. Gekelman, R. L. Stenzel, and N. Wild, Phys. Scr. **T2/2**, 277 (1982).
[11]R. L. Stenzel and W. Gekelman, Physica D **12**, 133 (1984).
[12]R. L. Stenzel and W. Gekelman, J. Geophys. Res. **86**, 649 (1981).
[13]W. Gekelman and R. L. Stenzel, J. Geophys. Res. **86**, 659 (1981).
[14]W. Gekelman, R. L. Stenzel, and N. Wild, J. Geophys. Res. **87**, 101 (1982).
[15]W. Gekelman and R. L. Stenzel, J. Geophys. Res. **89**, 2715 (1984).
[16]W. Gekelman and R. L. Stenzel, Phys. Rev. Lett. **54**, 2414 (1985).
[17]M. Yamada, Y. Ono, A. Hayakawa, M. Katsurai, and F. W. Perkins, Phys. Rev. Lett. **65**, 721 (1990).
[18]M. Yamada, F. W. Perkins, A. K. MacAulay, Y. Ono, and M. Katsurai, Phys. Fluids B **3**, 2379 (1991).
[19]Y. Ono, A. Morita, M. Katsurai, and M. Yamada, Phys. Fluids B **5**, 3691 (1993).
[20]Y. Ono, M. Yamada, T. Akao, T. Tajima, and R. Matsumoto, Phys. Rev. Lett. **76**, 3328 (1996).
[21]M. Yamada, H. Ji, S. Hsu, T. Carter, R. Kulsrud, Y. Ono, and F. Perkins, Phys. Rev. Lett. **78**, 3117 (1997).
[22]H. Ji, M. Yamada, S. Hsu, and R. Kulsrud, Phys. Rev. Lett. **80**, 3256 (1998).
[23]C. G. R. Geddes, T. W. Kornack, and M. R. Brown, Phys. Plasmas **5**, 1027 (1998).
[24]T. W. Kornack, P. K. Sollins, and M. R. Brown, Phys. Rev. E **58**, 36 (1998).
[25]H. Ji, H. Toyama, K. Yamagishi, S. Shinohara, A. Fujisawa, and K. Miyamoto, Rev. Sci. Instrum. **62**, 2326 (1991).